

The influence of size, clearance, cartilage properties, thickness and hemiarthroplasty on
the contact mechanics of the hip joint with biphasic layers

J Li¹, TD Stewart¹, Z Jin^{1,2}, RK Wilcox¹, J Fisher¹

Institute: ¹Institute of Medical and Biological Engineering, School of Mechanical Engineering, University of Leeds, UK

²School of Mechanical Engineering, Xi'an Jiaotong University, People's Republic of China

Key words: Contact mechanics, Articular cartilage, Biphasic, Hip, Finite element

Abstract

Computational models of the natural hip joint are needed to examine and optimise tissue sparing interventions where the natural cartilage remains part of the bearing surfaces. Although the importance of interstitial fluid pressurisation in the performance of cartilage has long been recognized, few studies have investigated the time dependent interstitial fluid pressurisation in a three dimensional natural hip joint model. The primary aim of this study was to develop a finite element model of the natural hip incorporating the biphasic cartilage layers that was capable of simulating the joint response over a prolonged physiological loading period. An initial set of sensitivity studies were also undertaken to investigate the influence of hip size, clearance, cartilage properties, thickness and hemiarthroplasty on the contact mechanics of the joint. The contact stress, contact area, fluid pressure and fluid support ratio were calculated and cross-compared between models with different parameters to evaluate their influence. It was found that the model predictions for the period soon after loading were sensitive to the hip size, clearance, cartilage aggregate modulus, thickness and hemiarthroplasty, while the time dependent behaviour over 3000 seconds was influenced by the hip clearance and cartilage aggregate modulus, permeability, thickness and hemiarthroplasty. The modelling methods developed in this study provide a basic platform for biphasic simulation of the whole hip joint onto which more sophisticated material models or other input parameters could be added in the future.

1 **Introduction**

2 Articular cartilage comprises two principal phases: a solid phase which includes
3 collagen fibrils and proteoglycan macromolecules, and a water-like fluid phase. The
4 importance of interstitial fluid pressurisation on the behaviour of cartilage has been known
5 for decades (Mow et al., 1980, Mow et al., 1984, Ateshian et al., 1994). It has been proven
6 that osteoarthritis (OA) is related to not only the magnitude but also the duration of contact
7 stress (Hadley et al., 1990, Maxian et al., 1995), both of which are closely linked to the
8 mechanical behaviour of the interstitial fluid in the cartilage (Ateshian et al., 1994). In order
9 to study the biotribology of articular joints such as the hip, and to understand the changes that
10 occur with degeneration and potential interventions, it is therefore necessary to consider the
11 biphasic nature of the cartilage within the joint system.

12 Experimental measurements of articular joint contact mechanics can provide valuable
13 information, but they involve highly invasive techniques such as the insertion of transducers
14 (Brown and Shaw, 1983, Hodge et al., 1989) or pressure-sensitive film (Afoke et al., 1987)
15 into the joint. These methods may introduce measurement artefacts between articular surfaces
16 and thus affect the results (Brand et al., 2001). Moreover, the parameters that can be
17 measured are limited. For instance, direct measurement of fluid pressure distribution inside
18 the cartilage of the natural hip joint is currently difficult and has only been achieved for very
19 simple configurations (Soltz and Ateshian, 1998, Park et al., 2003).

20 Numerical analysis serves as an alternative approach. However, existing models
21 assume the cartilage to be either elastic or hyperelastic (Yoshida et al., 2006, Anderson et al.,
22 2008, Chegini et al., 2009, Anderson et al., 2010, Harris et al., 2012), which cannot account
23 for the interstitial fluid flow in the cartilage. The loss of load support by the fluid in the
24 cartilage is believed to be one reason for the increased coefficient of friction and higher shear
25 stress which may lead to progressive degradation in the cartilage and onset of hip OA
26 (Forster and Fisher, 1996, McCann et al., 2009). Biphasic modelling is able to account for the
27 fluid flow in the cartilage providing more information on the contact mechanics and tribology
28 for the natural hip joint. Several numerical studies on the investigation of the labrum have
29 adopted biphasic soft tissues for two dimensional hip models (Ferguson et al., 2000a,
30 Ferguson et al., 2000b, Haemer et al., 2012). Recently, Pawaskar et al. (2010) developed a
31 three dimensional hemiarthroplasty hip model incorporating biphasic cartilage layers on the
32 acetabulum using Abaqus (version 6.7-1, DassaultSystemes, SuresnesCedex, France) and

33 applied the model to the simulation of daily activities for several cycles. However, for
34 biphasic cartilage-on-cartilage contact, especially in the case of whole joints, there are
35 difficulties in sustaining convergence of the model for prolonged periods of physiological
36 loading using this software. As yet, the biphasic approach does not appear to have been
37 applied to three dimensional modelling of the natural hip joint to examine the contact
38 mechanics over a prolonged physiological period of loading.

39 It is widely realized that the congruence and size of the human hip joint and the
40 material properties of the hip cartilage vary between individuals (Athanasίου et al., 1994, von
41 Eisenhart et al., 1999, Shepherd and Seedhom, 1999, Xi et al., 2003). However, to what
42 extent and how these parameters influence the contact mechanics of the natural hip joint are
43 not fully understood. Besides, the influence of hemiarthroplasty (e.g. femoral head replaced
44 with metallic prosthesis if only the femoral head cartilage breaks down (Pawaskar, 2010)) on
45 the hip function under prolonged physiological periods of loads is unclear. Quantifying these
46 influences can serve to better understand the hip function as well as to identify the accuracy
47 of measurements needed for the development of future subject-specific computational models
48 of the hip and their validation.

49 The primary aim of this study was therefore to develop a finite element (FE) model of
50 the natural hip incorporating the biphasic cartilage layers that was capable of simulating the
51 joint response over a prolonged physiological loading period. In order to investigate the role
52 of the parameters within this model, a set of sensitivity studies were then undertaken to
53 evaluate the influence of hip size, clearance, cartilage properties, thickness and
54 hemiarthroplasty on the contact mechanics of the joint.

55

56

57 **Methods**

58 The model utilized in the study was based on a standardized solid model of the pelvis
59 and femur from a 38 year-old healthy human male at the time of death, available from the
60 Internet through the BEL repository (Author: Vicceconti, from: www.tecno.ior.it/VRLAB/).
61 The acetabulum and the femoral head surfaces were carefully trimmed spherically
62 (Hammond and Charnley, 1967, Rushfeldt et al., 1981), and a layer of cartilage with uniform

63 thickness was created from the spherical area. The resultant model approximated the native
64 horseshoe shaped acetabular cartilage and the femoral head cartilage coverage (Figure 1).
65 The geometric model and corresponding FE model were generated using NX I-DEAS
66 (Version 6.1, Siemens PLM Software Inc., Plano, USA). The bone components of the femur
67 and pelvis were meshed with around 135,000 four-noded tetrahedral elements. The femoral
68 head and acetabular cartilage layers were made up of around 5700 and 8400 eight-noded
69 hexahedral elements respectively. The bone was meshed based on the elements of the
70 acetabular cartilage so that the surface of the subchondral bone shared the same nodes as the
71 inner surface of the cartilage layer. The mesh density was evaluated to ensure that the
72 differences in the peak contact stress, peak fluid pressure and fluid support ratio (the load
73 supported by the fluid pressure over the total load) were less than 5% when the number of
74 elements was doubled.

75 The material properties and geometric parameters associated with the cartilage were
76 initially taken from the literature and were then sequentially varied in a parametric study
77 (Table 1). The models with varied geometric parameters (i.e. size, clearance or cartilage
78 thickness) were achieved by scaling the spherically trimmed femur and pelvis and
79 subsequently recreating the cartilage layers. A hemiarthroplasty model was also generated
80 which had identical geometric parameters to the original model, with the femoral head
81 replaced by an impermeable sphere representing a metal prosthesis. The cartilage was
82 modelled as a biphasic solid and the solid phase was represented as neo-Hookean, with the
83 following strain energy (W) given in (Maas and Weiss, 2007).

$$84 \quad W = \frac{\mu}{2}(I_1 - 3) - \mu \ln J + \frac{\lambda}{2}(\ln J)^2$$

85 Where, μ and λ are the Lamé parameters; J volume ratio; I_1 first strain invariant of the
86 deviatoric Cauchy-Green tensor C .

87 The methodology and material constitutive relationship was verified on an indentation
88 model against a linearly elastic material model developed in ABAQUS (Pawaskar, 2010), and
89 both predicted similar time-dependent behaviour (Figure 2). The Poisson's ratio of the
90 aggregate was 0.045; this value has been shown to have little influence on the results when
91 varied from 0 to 0.1 (Athanasίου et al., 1994).

92 The bone was modelled as impermeable and linearly elastic with a Young's modulus of
93 17000 MPa and Poisson's ratio of 0.3 (Dalstra and Huiskes, 1995). The cortical bone and
94 trabecular bone were not modelled separately because it was found that changes in the peak
95 contact stress and peak fluid pressure were within 5% if the Young's modulus of the whole
96 region was reduced from that representing all cortical bone (17000 MPa) to that representing
97 all trabecular bone (800 MPa).

98 Nodes at the sacroiliac and pubis symphysis joints were fixed in all degrees of freedom.
99 The contact between articulating surfaces was assumed to be frictionless. For the models of
100 natural joints, the contact formulation allowed fluid to flow between contacting surfaces as
101 well as from open surfaces of the cartilage. No fluid flow was allowed through the contact-
102 against-rigid surfaces of the acetabular cartilage in the hemiarthroplasty model. A static load
103 of approximately 2130 N, based on the average data for one leg stance (Bergmann et al.,
104 2001), was applied to the distal femur, which was constrained in rotational degrees of
105 freedom. The load was ramped over 0.6 seconds and then held constant for 3000 seconds.

106 All analyses were conducted using the open-source nonlinear FE solver FEBio (version
107 1.5.0; mrl.sci.utah.edu/software/febio) (Maas et al., 2012) due to its good convergence ability
108 in the simulation of biphasic materials in contact. The models were solved on a Linux server
109 with 8 GB of RAM and 8 Intel X5560 cores at 2.8 GHz. Contact stress, contact area, fluid
110 pressure and fluid support ratio were recorded over the time period from 0 to 3000 seconds to
111 evaluate the load transmission and tribological performance.

112

113

114 **Results**

115 As an example, the fluid pressure distribution and contact stress of the original model
116 are presented in Figure 3. Over the acetabular cartilage surface, the contact stress and fluid
117 pressure peaked around the centre of the cartilage and decreased gradually towards the edges.
118 The contact stress and fluid pressure contours on both the femoral head and the acetabular
119 cartilage surfaces of the natural hips were very similar. The peak fluid pressure was slightly
120 lower than the peak contact stress over 3000 seconds for all the models (Figure 4). There was
121 no marked difference in the fluid pressure across the thickness of the cartilage (Figure 5). The

122 contact area was calculated as a ratio of the total surface area (3000 mm² for the original
123 model) of the acetabular cartilage available for articulation.

124 The results of the parametric studies are shown in Figure 4. At the end of 1 second, the
125 models with smaller size, larger clearance, stiffer cartilage aggregate, thinner cartilage or
126 hemiarthroplasty had higher peak contact stress, higher peak fluid pressure and smaller
127 absolute contact area. For all the models, the peak contact stress lay between 2.7 MPa and 4.1
128 MPa; the contact area ranged from 42% to 66%; and fluid supported 93% to 99% of the
129 loads. At this early period after loading, the models with different cartilage permeabilities had
130 nearly identical results.

131 Over the period of 3000 seconds, there was a decrease in the peak fluid pressure and the
132 fluid support ratio for all the models. The models with larger size, stiffer cartilage aggregate,
133 higher cartilage permeability, larger clearance, thinner cartilage or hemiarthroplasty had a
134 greater decrease in the peak fluid pressure (Figure 4). There was a decrease of over 10% in
135 the peak fluid pressure for the models with 1.8 MPa cartilage Young's modulus, 0.00143
136 mm⁴/Ns cartilage permeability, 1 mm clearance and 1 mm thick cartilage, as well as the
137 hemiarthroplasty case. Generally, the models with higher change in the peak fluid pressure
138 also had higher change in the peak contact stress and contact area over 3000 seconds. For all
139 the models, the reduction in the fluid support ratio was minimal and less than 5% even after
140 3000 seconds. As compared to the other parameters, changes in the fluid support ratio were
141 most sensitive to the variation in cartilage permeability.

142

143

144 **Discussion**

145 In this study, a model of the whole natural hip with biphasic cartilage-on-cartilage and
146 cartilage-on-solid contact was developed. Whilst such models have been employed
147 previously for more simple geometry with two dimensions (Wu et al., 1997, Ferguson et al.,
148 2000a, Ferguson et al., 2000b, Haemer et al., 2012), there are several challenges in
149 representing the whole three dimensional joint and simulating the contact behaviour,
150 particularly over a prolonged physiological period of loading. The approach taken in this
151 study was to use FEBio to solve the models instead of Abaqus which has been used
152 previously for the simulation of biphasic materials such as cartilage (Ferguson et al., 2000a,

153 Ferguson et al., 2000b, Pawaskar et al., 2010, Manda et al., 2011). For contact problems with
154 biphasic materials, the FEBio solver was able to achieve convergence in the simulation of the
155 whole joint with biphasic cartilage on cartilage contact even over a prolonged period, which
156 was not possible with other FE solvers. For example, Pawaskar (2010) employed Abaqus to
157 simulate both the natural hip joint and the hip joint with hemiarthroplasty incorporating
158 biphasic cartilage properties. Whilst the hemiarthroplasty model, which involved a rigid body
159 on biphasic cartilage contact, could be simulated for 600 seconds under a static load, the
160 natural joint model, also with spherical articulating surfaces, could only be solved for one
161 second under a ramped load, due to convergence difficulties.

162 In this study, for the solid phase, a neo-Hookean model was adopted for practical
163 reasons because the linearly elastic material within a biphasic model does not perform well
164 with the non-linear FE solver in FEBio. This difference in material model is unlikely to affect
165 the results because, across the range of strains seen in this study, it was found that the
166 cartilage with a neo-Hookean solid phase in FEBio behaves nearly identically to the linearly
167 elastic solid phase model in ABAQUS in terms of the stress, strain and fluid pressure
168 distribution (Figure 2) (Maas and Weiss, 2007).

169 The primary aim of this study was to develop the necessary modelling methodology for
170 simulating the natural hip over prolonged physiological periods. Whilst this was achieved,
171 there were some limitations. In reality, as well as being biphasic, the cartilage layer is an
172 inhomogenous fiber-reinforced structure (Mow et al., 1980, Soulhat et al., 1999, Ateshian et
173 al., 2009), and the homogenous isotropic elastic model used here as a first approximation
174 does not fully represent its behaviour. Although the 3000 seconds adopted in this study
175 represents a relatively long physiological loading period, the cartilage behaviour is still
176 relatively early in the transient phase and the results against time had not yet reached the
177 equilibrium state that can be observed eventually in creep tests (Mow et al., 1980, Athanasiou
178 et al., 1994). In terms of capturing the early stage response of creep tests, a tension-
179 compression non-linear model (Soltz and Ateshian, 2000, Cohen et al., 1993, Cohen et al.,
180 1998) may be more appropriate than the linear isotropic biphasic model used in this study
181 (Mow et al., 1989, Mow et al., 1980). In addition, the choice of linear isotropic material
182 properties for the cartilage neglects the fact that the tensile modulus of the cartilage is
183 substantially higher than its aggregate modulus (Soltz and Ateshian, 2000). This could reduce
184 the confinement effect due to the tensile stiffness. Consequently, the peak fluid pressure, peak
185 contact stress and fluid support ratio may be underestimated. The influence of cartilage

186 thickness may also be amplified since here the confinement is provided more by the
187 underlying bone geometry. Further development of this model will focus on the
188 implementation of tension-compression non-linear solid phase into the whole joint model in
189 order to evaluate these effects in more detail.

190 The congruence, size and material properties of the hip joint vary between individuals.
191 The parametric study was therefore undertaken as a precursor to future model validation to
192 identify the sensitivity of the model to these parameters. The findings of this study show that
193 the contact mechanics of the hip joint are dependent on its congruence, size, cartilage
194 thickness and properties as well as the contact type (i.e. cartilage-on-cartilage and cartilage-
195 on-solid). Over the ranges studied here, the thickness and clearance were found to have the
196 greatest effect on the contact mechanics. This is in agreement with the sensitivity study of
197 Anderson et al. (2010) in an elastic model, where it was found that the cartilage thickness and
198 local surface morphology had a major effect on the contact stress and distribution. Whilst the
199 effect of the thickness may be overestimated by the simplified material model used, it is a
200 parameter that needs to be taken into consideration in future sensitivity studies and subject-
201 specific modelling.

202 The influence of the cartilage material properties was generally less than that of the
203 morphology. In particular, the effect of the cartilage permeability on the contact mechanics of
204 the hip joint was minimal during the early stages, but became evident after a period of load.
205 The fluid support ratio was more sensitive to the cartilage thickness than other parameters at
206 an early period because, as shown in Figure 4, the hip congruence at this stage is highly
207 related to the cartilage thickness as well as the clearance. For the model with thicker
208 cartilage, the contact stress was spread more towards the area near the edge of the cartilage
209 which is less confined than around the central region, leading to a lower fluid support ratio.
210 This is because the fluid support ratio of the cartilage under unconfined compression is
211 substantially lower than that under confined compression (Park et al., 2003, Ateshian and
212 Hung, 2006). However, in reality, such differences may be reduced by the tension-
213 compression nonlinearity of the cartilage. The hemiarthroplasty case showed higher peak
214 stresses and a greater reduction in the fluid-load support over time than the cartilage-on-
215 cartilage case. This illustrates that it is necessary to model both layers of cartilage to represent
216 the natural joint since their interaction plays an important role in the contact mechanics.

217 For models with different parameters presented in this study, the predicted peak contact
218 stress was found to range from 2.7 to 4.1 MPa. For similar loading conditions, the peak
219 contact stress has been reported to lie between 4 MPa and 7 MPa in a study using embedded
220 transducers (Brown and Shaw, 1983, Hodge et al., 1989)) and between 5 MPa and 10 MPa in
221 studies using pressure-sensitive films (Afoke et al., 1987, Anderson et al., 2008). Besides the
222 linear isotropic assumption of the cartilage, the higher values of such measurements could be
223 because the film thickness and stiffness introduce measurement artefacts, but also because of
224 the smooth surfaces and regular morphology assumptions in this study, which have been
225 shown to reduce the peak contact stress in an elastic FE model (Anderson et al., 2010). The
226 peak stress predictions in this study are consistent with previous numerical studies where
227 similar spherical assumptions have been made (i.e. 3 MPa to 4 MPa) (Mavčič et al., 2002,
228 Yoshida et al., 2006, Pawaskar et al., 2010). For the purpose of the current study, the
229 spherical assumption was necessary in order to undertake the initial parametric study and
230 gain an understanding of the order of importance of the model input conditions. In order to
231 directly validate the results against experiment using subject-specific models, it is clear that
232 the individual variations in the morphology of the cartilage are important.

233 The labrum was excluded in this study due to a lack of extensive literature on its
234 geometric parameters and material properties (Anderson et al., 2008), which is another
235 potential limitation. Although the labrum plays a minimal role in load supporting for the
236 normal hip (1-2% of total load) (Henak et al., 2011), it is believed to help impede the fluid
237 exudation, owing to its lower permeability compared with the cartilage (Ferguson et al.,
238 2000a, Ferguson et al., 2000b, Ferguson et al., 2003, Haemer et al., 2012). After labrum
239 removal, the edge surface of the acetabular cartilage remains free-draining, potentially
240 leading to a faster process of fluid exudation compared with a hip with the labrum. The
241 findings in this study illustrate that even under the extreme situation where the labrum is
242 removed, the fluid supports most of the load over prolonged physiological loading periods,
243 further demonstrating the excellent function of the hip joint.

244 The primary advantage of the methodology in this study lies in its ability to investigate
245 the solid phase and fluid phase separately, predict the joint tribological behaviour under both
246 short-term and long-term loading periods, and interpret the influence of model parameters on
247 the fluid-solid phases over prolonged physiological loading periods. Due to the importance of
248 interstitial fluid in cartilage function and degeneration particularly over long-term loading
249 periods (Mow et al., 1980, Mow et al., 1984, Ateshian et al., 1994), this modelling approach

250 could allow further investigation of the functional and tribological behaviour of the joint and
251 the pathology of joint degeneration. The results predicted by this study illustrate how the
252 cartilage geometry and structure aid in the function of the natural hip joint. The soft and
253 conforming contact surfaces ensure a large contact area and low peak contact stress, despite a
254 high load being applied. Owing to the good congruence of the hip joint and the very low
255 cartilage permeability, fluid exudation occurs slowly and the fluid supported most of the load
256 even under extreme situations (e.g. 3000 seconds), leaving a small portion of load transferred
257 to the solid phase of the cartilage and the solid-solid contact which would reduce the
258 frictional coefficient and shear stress in reality (Krishnan et al., 2004).

259 In conclusion, in the present study a new method for simulating the contact mechanics
260 and associated fluid pressurisation for a biphasic natural hip joint under prolonged
261 physiological loading was presented. The predicted behaviour of the natural hip joint model
262 was found to be subject to hip size, clearance, cartilage aggregate modulus, thickness and
263 hemiarthroplasty for the period soon after loading. The fluid in the cartilage supports over
264 90% of the load transmitted between the articulating surfaces of the hip joint for a prolonged
265 physiological loading period. The model with higher congruence or lower cartilage
266 permeability has slower changes over this period. These findings are important for planning
267 future subject-specific modelling approaches. Whilst there were some simplification to the
268 material model and geometry used in this study, the methods presented provide a basic
269 platform and initial understanding of the sensitivity of the model onto which more
270 sophisticated material models and geometric parameters could be added in the future. This
271 computational approach has the potential to aid in understanding the mechanisms of hip
272 function and the pathology of hip degeneration.

273

274

275 **Acknowledgements:**

276 The research was supported by the EPSRC, the Centre of Excellence in Medical
277 Engineering funded by the Wellcome Trust and EPSRC WT 088908/z/09/z and by the NIHR
278 LMBRU Leeds Musculoskeletal Biomedical Research Unit. JF is an NIHR senior
279 investigator.

280

281 Word count (from the Introduction through the Acknowledgement including any appendices):
282 3597

283

284 **Reference:**

- 285 AFOKE, N. Y., BYERS, P. D. & HUTTON, W. C. 1987. Contact pressures in the human hip joint. *Journal*
286 *of Bone and Joint Surgery (British)*, 69, 536-41.
- 287 ANDERSON, A. E., ELLIS, B. J., MAAS, S. A., PETERS, C. L. & WEISS, J. A. 2008. Validation of finite
288 element predictions of cartilage contact pressure in the human hip joint. *Journal of*
289 *Biomechanical Engineering*, 130, 051008.
- 290 ANDERSON, A. E., ELLIS, B. J., MAAS, S. A. & WEISS, J. A. 2010. Effects of idealized joint geometry on
291 finite element predictions of cartilage contact stresses in the hip. *Journal of Biomechanics*,
292 43, 1351-1357.
- 293 ATESHIAN, G. A. & HUNG, C. T. 2006. The natural synovial joint: Properties of cartilage. *Proceedings*
294 *of the Institution of Mechanical Engineers, Part J: Journal of Engineering Tribology*, 220, 657-
295 670.
- 296 ATESHIAN, G. A., LAI, W. M., ZHU, W. B. & MOW, V. C. 1994. An asymptotic solution for the contact
297 of two biphasic cartilage layers. *Journal of Biomechanics*, 27, 1347-1360.
- 298 ATESHIAN, G. A., RAJAN, V., CHAHINE, N. O., CANAL, C. E. & HUNG, C. T. 2009. Modeling the matrix
299 of articular cartilage using a continuous fiber angular distribution predicts many observed
300 phenomena. *Journal of Biomechanical Engineering*, 131, 061003.
- 301 ATHANASIOU, K. A., AGARWAL, A. & DZIDA, F. J. 1994. Comparative study of the intrinsic mechanical
302 properties of the human acetabular and femoral head cartilage. *Journal of Orthopaedic*
303 *Research*, 12, 340-349.
- 304 BERGMANN, G., DEURETZBACHER, G., HELLER, M., GRAICHEN, F., ROHLMANN, A., STRAUSS, J. &
305 DUDA, G. N. 2001. Hip contact forces and gait patterns from routine activities. *Journal of*
306 *Biomechanics*, 34, 859-871.
- 307 BRAND, R., IGLIC, A. & KRALJ-IGLIC, V. 2001. Contact stresses in the human hip: implications for
308 disease and treatment. *Hip International*, 11, 117-126.
- 309 BROWN, T. D. & SHAW, D. T. 1983. In vitro contact stress distributions in the natural human hip.
310 *Journal of Biomechanics*, 16, 373-384.
- 311 CHEGINI, S., BECK, M. & FERGUSON, S. J. 2009. The Effects of Impingement and Dysplasia on Stress
312 Distributions in the Hip Joint during Sitting and Walking: A Finite Element Analysis. *Journal of*
313 *Orthopaedic Research*, 27, 195-201.
- 314 COHEN, B., GARDNER, T. R. & ATESHIAN, G. A. 1993. The influence of transverse isotropy on cartilage
315 indentation behavior - A study of the human humeral head. *Transactions on Orthopaedic*
316 *Research Society*, 18, 185.
- 317 COHEN, B., LAI, W. M. & MOW, V. C. 1998. A transversely isotropic biphasic model for unconfined
318 compression of growth plate and chondroepiphysis. *Journal of Biomechanical Engineering*,
319 120, 491-496.
- 320 DALSTRA, M. & HUISKES, R. 1995. Load transfer across the pelvic bone. *Journal of Biomechanics*, 28,
321 715-724.
- 322 FERGUSON, S. J., BRYANT, J. T., GANZ, R. & ITO, K. 2000a. The acetabular labrum seal: a poroelastic
323 finite element model. *Clinical Biomechanics*, 15, 463-468.
- 324 FERGUSON, S. J., BRYANT, J. T., GANZ, R. & ITO, K. 2000b. The influence of the acetabular labrum on
325 hip joint cartilage consolidation: a poroelastic finite element model. *Journal of Biomechanics*,
326 33, 953-960.

327 FERGUSON, S. J., BRYANT, J. T., GANZ, R. & ITO, K. 2003. An in vitro investigation of the acetabular
328 labral seal in hip joint mechanics. *Journal of Biomechanics*, 36, 171-178.

329 FORSTER, H. & FISHER, J. 1996. The influence of loading time and lubricant on the friction of articular
330 cartilage. *Proceedings of the Institution of Mechanical Engineers, Part H: Journal of*
331 *Engineering in Medicine*, 210, 109-119.

332 HADLEY, N. A., BROWN, T. D. & WEINSTEIN, S. L. 1990. The effects of contact pressure elevations and
333 aseptic necrosis on the long-term outcome of congenital hip dislocation. *Journal of*
334 *Orthopaedic Research*, 8, 504-513.

335 HAEMER, J. M., CARTER, D. R. & GIORI, N. J. 2012. The low permeability of healthy meniscus and
336 labrum limit articular cartilage consolidation and maintain fluid load support in the knee and
337 hip. *Journal of Biomechanics*, 45, 1450-1456.

338 HAMMOND, B. & CHARNLEY, J. 1967. The sphericity of the femoral head. *Medical and Biological*
339 *Engineering and Computing*, 5, 445-453.

340 HARRIS, M. D., ANDERSON, A. E., HENAK, C. R., ELLIS, B. J., PETERS, C. L. & WEISS, J. A. 2012. Finite
341 element prediction of cartilage contact stresses in normal human hips. *Journal of*
342 *Orthopaedic Research*, 30, 1133-1139.

343 HENAK, C. R., ELLIS, B. J., HARRIS, M. D., ANDERSON, A. E., PETERS, C. L. & WEISS, J. A. 2011. Role of
344 the acetabular labrum in load support across the hip joint. *Journal of Biomechanics*, 44,
345 2201-2206.

346 HODGE, W. A., CARLSON, K. L., FIJAN, R. S., BURGESS, R. G., RILEY, P. O., HARRIS, W. H. & MANN, R.
347 W. 1989. Contact pressures from an instrumented hip endoprosthesis. *Journal of Bone and*
348 *Joint Surgery (American)*, 71, 1378-86.

349 KRISHNAN, R., KOPACZ, M. & ATESHIAN, G. A. 2004. Experimental verification of the role of
350 interstitial fluid pressurization in cartilage lubrication. *Journal of Orthopaedic Research*, 22,
351 565-570.

352 MAAS, S. A., ELLIS, B. J., ATESHIAN, G. A. & WEISS, J. A. 2012. FEBio: Finite Elements for
353 Biomechanics. *Journal of Biomechanical Engineering*, 134, 011005.

354 MAAS, S. A. & WEISS, J. A. 2007. *FEBio Theory Manual*, <http://mrl.sci.utah.edu/software/febio>.

355 MANDA, K., RYD, L. & ERIKSSON, A. 2011. Finite element simulations of a focal knee resurfacing
356 implant applied to localized cartilage defects in a sheep model. *Journal of Biomechanics*, 44,
357 794-801.

358 MAVČIČ, B., POMPE, B., ANTOLIČ, V., DANIEL, M., IGLIČ, A. & KRALJ-IGLIČ, V. 2002. Mathematical
359 estimation of stress distribution in normal and dysplastic human hips. *Journal of Orthopaedic*
360 *Research*, 20, 1025-1030.

361 MAXIAN, T. A., BROWN, T. D. & WEINSTEIN, S. L. 1995. Chronic stress tolerance levels for human
362 articular cartilage: Two nonuniform contact models applied to long-term follow-up of CDH.
363 *Journal of Biomechanics*, 28, 159-166.

364 MCCANN, L., INGHAM, E., JIN, Z. & FISHER, J. 2009. Influence of the meniscus on friction and
365 degradation of cartilage in the natural knee joint. *Osteoarthritis and Cartilage*, 17, 995-1000.

366 MOW, V. C., GIBBS, M. C., LAI, W. M., ZHU, W. B. & ATHANASIOU, K. A. 1989. Biphasic indentation of
367 articular cartilage—II. A numerical algorithm and an experimental study. *Journal of*
368 *Biomechanics*, 22, 853-861.

369 MOW, V. C., HOLMES, M. H. & MICHAEL LAI, W. 1984. Fluid transport and mechanical properties of
370 articular cartilage: A review. *Journal of Biomechanics*, 17, 377-394.

371 MOW, V. C., KUEI, S. C., LAI, W. M. & ARMSTRONG, C. G. 1980. Biphasic creep and stress relaxation
372 of articular cartilage in compression: Theory and experiments. *Journal of Biomechanical*
373 *Engineering*, 102, 73-84.

374 PARK, S., KRISHNAN, R., NICOLL, S. B. & ATESHIAN, G. A. 2003. Cartilage interstitial fluid load support
375 in unconfined compression. *Journal of Biomechanics*, 36, 1785-1796.

376 PAWASKAR, S. S. 2010. *Joint contact modelling of articular cartilage in synovial joints*. Ph.D. Thesis,
377 University of Leeds.

378 PAWASKAR, S. S., INGHAM, E., FISHER, J. & JIN, Z. 2010. Fluid load support and contact mechanics of
379 hemiarthroplasty in the natural hip joint. *Medical Engineering and Physics*, 33, 96-105.

380 RUSHFELDT, P. D., MANN, R. W. & HARRIS, W. H. 1981. Improved techniques for measuring in vitro
381 the geometry and pressure distribution in the human acetabulum—I. Ultrasonic
382 measurement of acetabular surfaces, sphericity and cartilage thickness. *Journal of*
383 *Biomechanics*, 14, 253-260.

384 SHEPHERD, D. E. & SEEDHOM, B. B. 1999. Thickness of human articular cartilage in joints of the
385 lower limb. *Annals of the Rheumatic Diseases*, 58, 27-34.

386 SOLTZ, M. A. & ATESHIAN, G. A. 1998. Experimental verification and theoretical prediction of
387 cartilage interstitial fluid pressurization at an impermeable contact interface in confined
388 compression. *Journal of Biomechanics*, 31, 927-934.

389 SOLTZ, M. A. & ATESHIAN, G. A. 2000. A Conewise Linear Elasticity mixture model for the analysis of
390 tension-compression nonlinearity in articular cartilage. *Journal of Biomechanical*
391 *Engineering*, 122, 576-86.

392 SOULHAT, J., BUSCHMANN, M. D. & SHIRAZI-ADL, A. 1999. A fibril-network-reinforced biphasic
393 model of cartilage in unconfined compression. *Journal of Biomechanical Engineering*, 121,
394 340-7.

395 VON EISENHART, R., ADAM, C., STEINLECHNER, M., MULLER-GERBL, M. & ECKSTEIN, F. 1999.
396 Quantitative determination of joint incongruity and pressure distribution during simulated
397 gait and cartilage thickness in the human hip joint. *Journal of Orthopaedic Research*, 17, 532-
398 539.

399 WU, J. Z., HERZOG, W. & EPSTEIN, M. 1997. Evaluation of the finite element software ABAQUS for
400 biomechanical modelling of biphasic tissues. *Journal of Biomechanics*, 31, 165-169.

401 XI, J., HU, X. & JIN, Y. 2003. Shape analysis and parameterized modeling of hip joint. *Journal of*
402 *Computing and Information Science in Engineering*, 3, 260-265.

403 YOSHIDA, H., FAUST, A., WILCKENS, J., KITAGAWA, M., FETTO, J. & CHAO, E. Y. S. 2006. Three-
404 dimensional dynamic hip contact area and pressure distribution during activities of daily
405 living. *Journal of Biomechanics*, 39, 1996-2004.

406

407

Figure 1: The three-dimensional finite element model of the hip joint. A – The entire model, B – Lateral view of acetabulum. C – Oblique view of acetabular cartilage with hexahedral elements.

Figure 2: Verification of the constitutive properties (left – model; right – results). Indentation model of a creep test using a quarter-symmetry model. Material properties and geometric parameters were taken from a previous study (Pawaskar, 2010). The biphasic model with neo-Hookean solid phase in FEBio behaves nearly identically to the biphasic model with linearly elastic solid phase in ABAQUS (Maas and Weiss, 2007). The experimental results from Pawaskar (2010) are also shown.

Figure 3: Contours of fluid pressure (MPa) and contact stress (MPa) of the acetabular cartilage for the original model at 1 second and 3000 seconds. On the acetabular cartilage surface, the peak contact stress is slightly higher than the peak fluid pressure. Obvious cartilage consolidation can be detected. The change in the fluid pressure is greater than that in the contact stress.

Figure 4: The results of the parametric tests for all models at 1 second and 3000 seconds. Both the short-term and long-term behaviour of the models depend on the size, clearance, hemiarthroplasty, cartilage thickness and stiffness. Cartilage permeability has almost no influence on the short-term behaviour, but greatly affects the long-term performance of the model.

Figure 5: Cross-sectional view of fluid pressure (MPa) in the cartilage of the acetabulum (1) and femoral head (2) of the original model at 1 second. Fluid pressure distribution was similar for the femoral head cartilage and acetabular cartilage. There was no marked difference in the fluid pressure across the thickness of the cartilage.

Figure 1

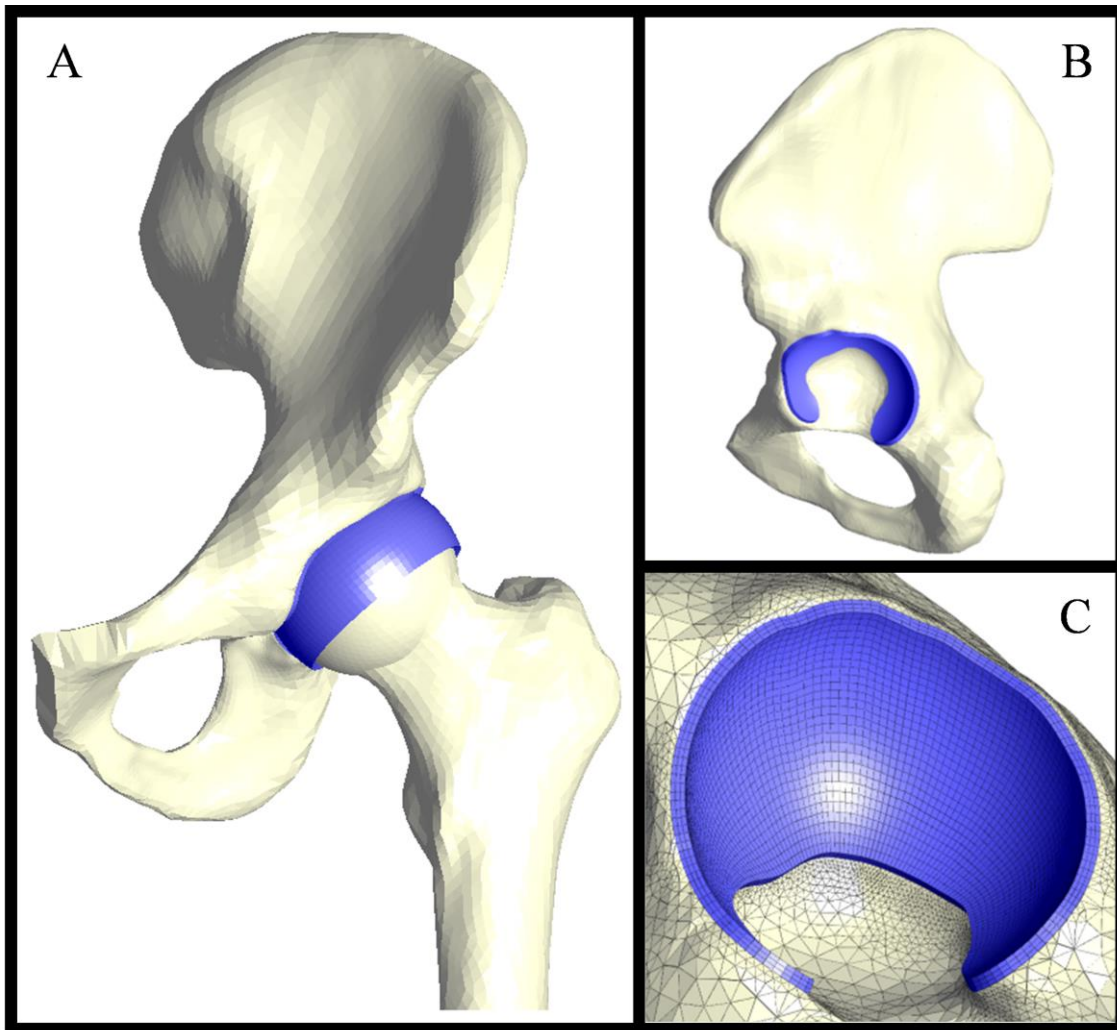


Figure 2

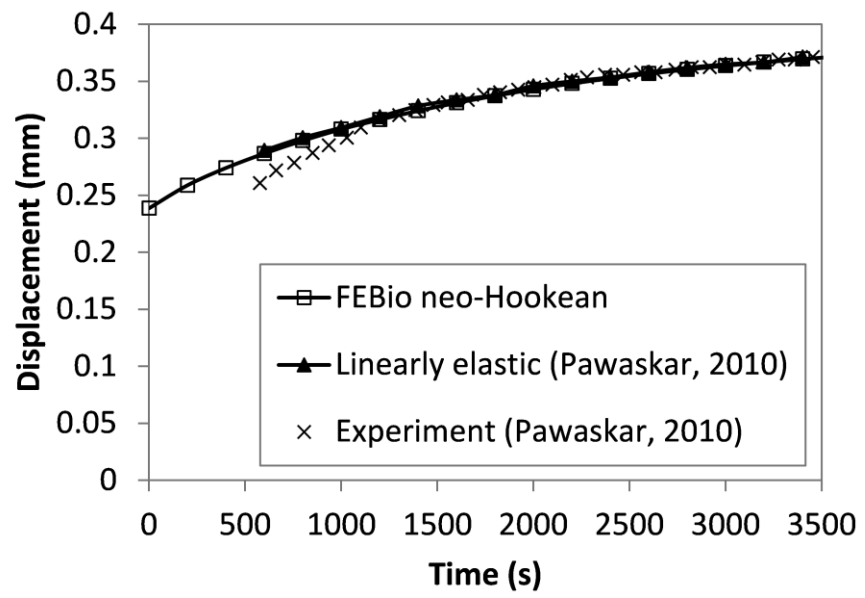
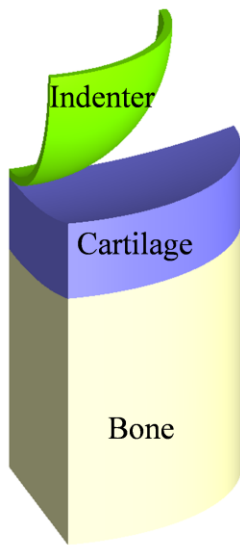


Figure 3

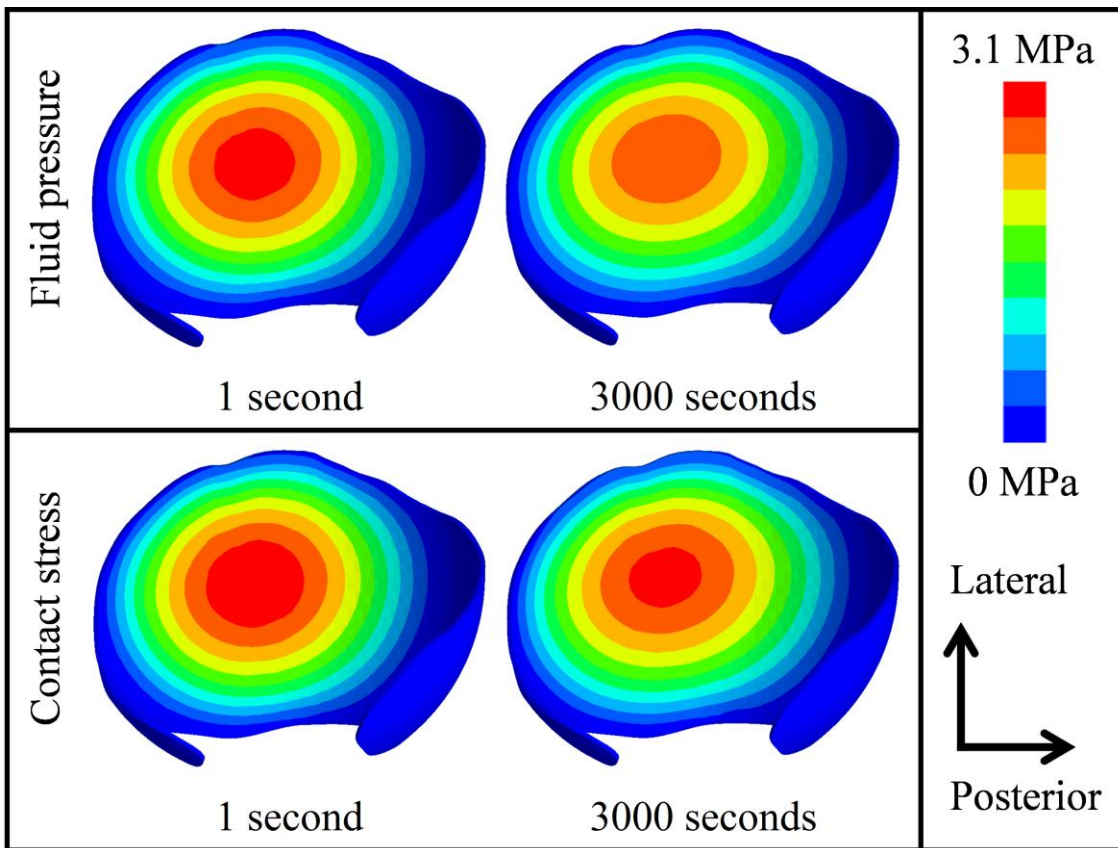


Figure 4

	Hemiarthroplasty / HA	E (MPa)	K (mm ⁴ /Ns)	Cl (mm)	Thick (mm)	Size (mm)
×	Yes	0.6	0.00036	0	1	26
Original	No	1.2	0.0009	0.5	2	30
□		1.8	0.00143	1	3	28

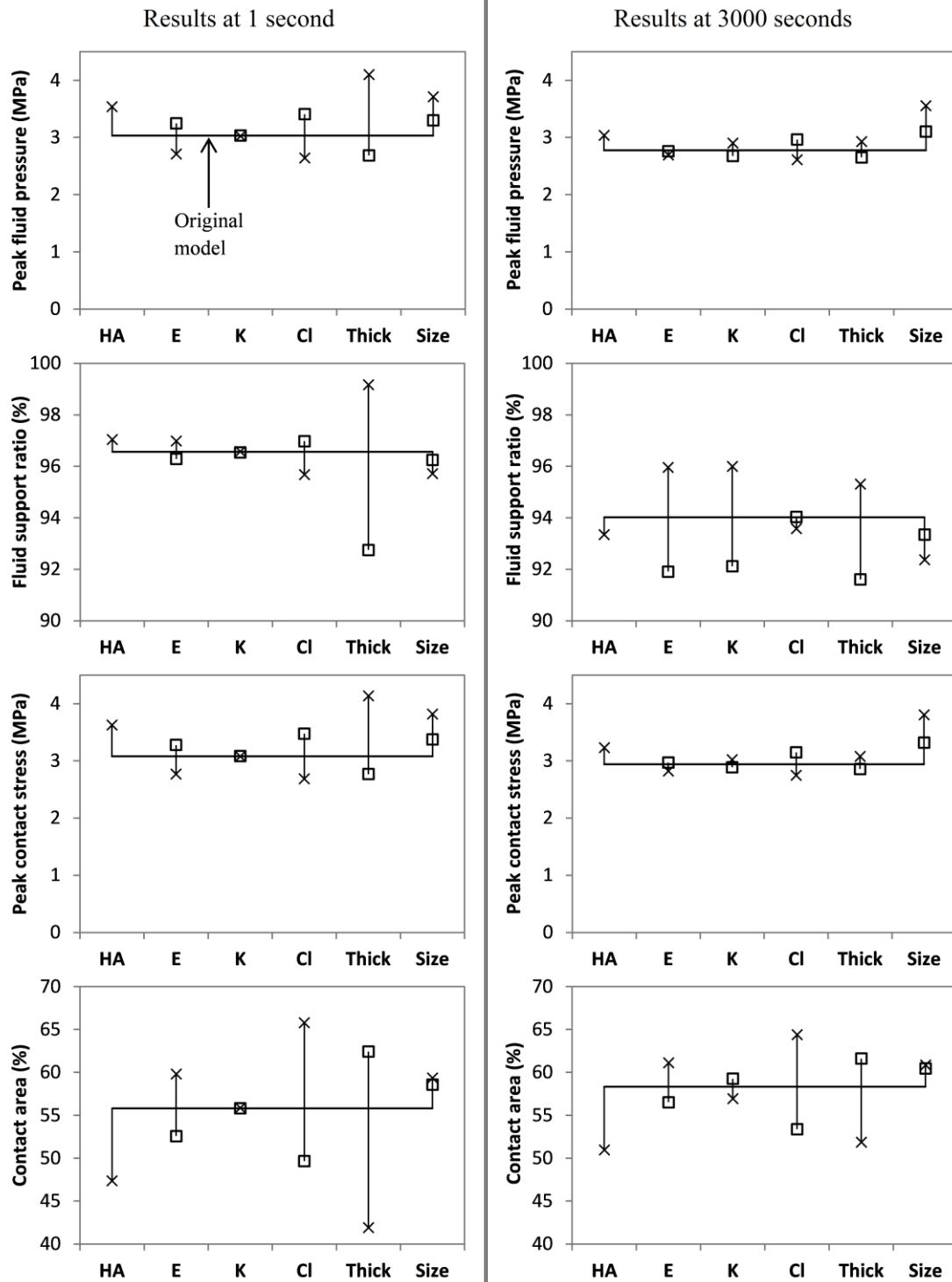


Figure 5

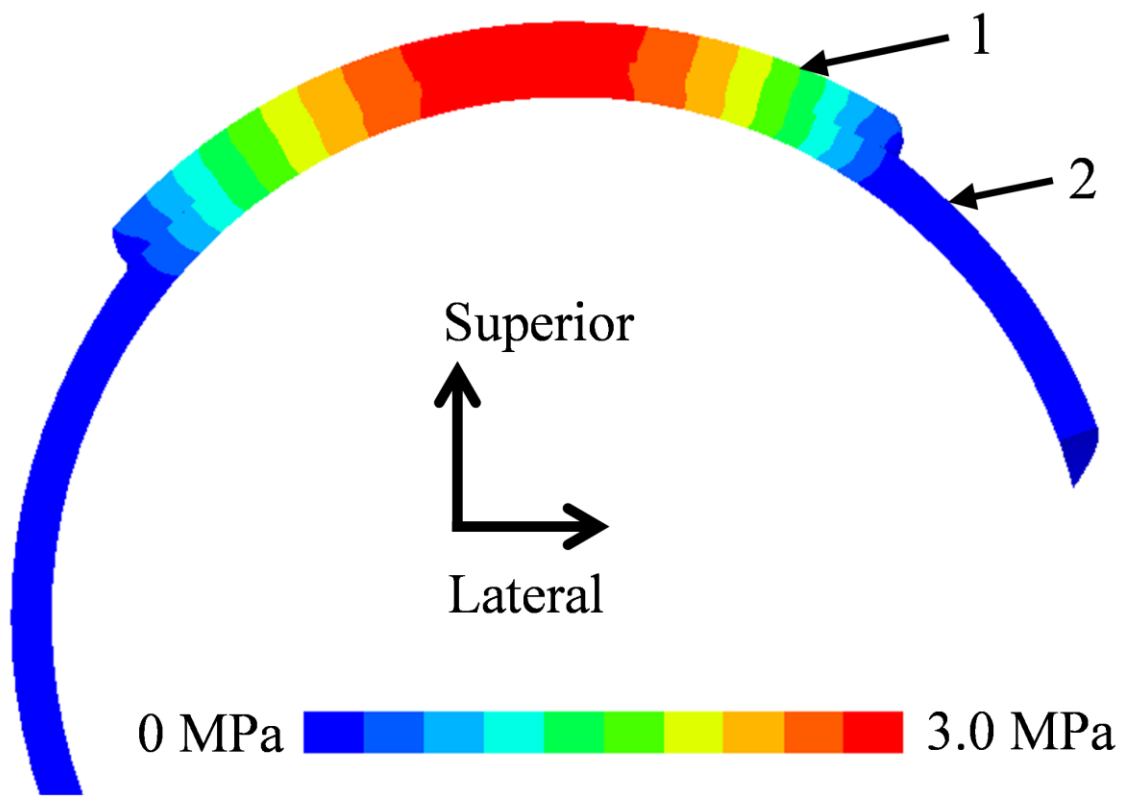


Table 1: The values of the parameters used in the original model and parametric tests. Only one parameter was altered from the original in each test case. E: Young’s modulus of cartilage aggregate; K: cartilage permeability; Cl: radial clearance; Size: acetabulum radius; Thick: cartilage thickness.

Model	E (MPa)	K (mm⁴/Ns)	Cl (mm)	Size (mm)	Thick (mm)
Original	1.2	0.0009	0.5	30	2
Values used in parametric studies	0.6, 1.8	0.00036, 0.00143	0, 1	26, 28	1, 3
References	(Athanasίου et al., 1994)		(von Eisenhart et al., 1999)	(Xi et al., 2003)	(Shepherd and Seedhom, 1999)